A&A 403, 413–418 (2003)
DOI: 10.1051/0004-6361:20030399

Astronomy & Astrophysics

The effect of falling particles on the shape and spin rate of an asteroid

O. Vasilkova

Pulkovo Astronomical Observatory, 65/1 Pulkovskoje shosse, 196140 St.-Petersburg, Russian;
Isaac Newton Institute of Chile, St. Petersburg Branch
e-mail: olyaov@mail.ru

Received 31 January 2002 / accepted 25 February 2003

Abstract. This simulation is focused on the specific influence of the gravitational field of a very elongated rotating asteroid on the location of zones of the most intensive bombardment by falling particles. It is assumed that the particles are distributed uniformly in the space surrounding the asteroid. The asteroid shape is approximated by a triaxial ellipsoid with semiaxes 28, 12, 10.5 km (equal to those of asteroid 243 Ida) and by a dumb-bell of the same mass. The computations and appropriate figures show that at a rotation period faster than approximately 9.1 hours for the triaxial ellipsoid model and 3.3 hours for the dumb-bell one the leading sides of the asteroid receive a higher flux of impacting particles than the trailing sides while at slower periods the situation is the opposite. The zones of possible erosion are computed depending on the asteroid rotation period and on the ratio of impact and rebound velocities of particles. The contribution of all impacting particles to the angular momentum of the asteroid is computed, which leads to the conclusion that falling out of particles damps the asteroid rotation at any spin period.

Key words. celestial mechanics – methods: numerical – minor planets, asteroids – solar system: general

1. Introduction

Original asteroid parent bodies are not spherical. Produced by low-velocity collisions, they could form rubble-piles of an equilibrium ellipsoidal shape or dumb-bell shaped compound planetesimals (Bell et al. 1989). This paper presents a simulation that is the first-order approximation to understand how asteroid planetesimals of such elongated shape grew during the early accretion stage. It concentrates on the effect of the nonspherical shape of the asteroid on the distribution of areas subjected to the most intensive bombardment by impacting particles.

The following assumptions were made. All particles are of the same mass and distributed uniformly inside of a spherical layer of 200 to 1000 km surrounding an asteroid of a very elongated shape (triaxial ellipsoid with semiaxes 28, 12 and 10.5 km and a dumb-bell of the same mass). The particles are not so small (of the order of a meter in diameter) as to be subjected to gas drag, the Pointing-Robertson effect or radiation pressure. On the other hand, the mass of particles is not too large to perturb either the gravitational field of the asteroid or the motion of particles due to their mutual interactions.

The early accretionary stage is considered here when the orbits of particles and bodies were near-circular, relative velocities were low and the Jupitor core was not large enough to perturb the growing planetesimals (Safronov 1972; Hartmann 1968; Ruskol & Safronov 1998, etc.). Under these conditions the zero initial velocities of particles (with respect to the center of the asteroid) adopted in the current simulation are justified, as well as the meter sizes of falling particles which seem to be proper for the early accretionary stage when in the absence of crushing of bodies (due to very low velocities), small particles were mostly swept out by the larger bodies, and the cloud transformed into a swarm. At this point, the further process of growth consisted principally of the fall of individual bodies onto the embryos (Safronov 1958, 1972). When close to an asteroid planetesimal, the gravitational attraction and perturbations due to deviation of the body's shape from the spherical dominates the other perturbations such as solar tide, solar radiation pressure, perturbations from the planets, gas drag and the Pointing-Robertson effect, especially as the particles of the size chosen are not as sensitive to perturbations concerned with solar radiation or gas drag as the smaller ones.

In the simulation a time span of only a few days is considered that allows us to neglect the perturbations above. In a complete model monitored during a few asteroid revolutions around the sun and including a more realistic power law size distribution of falling particles, all the perturbations above should be considered. Also, interaction of the particles with each other, their own spinning, unevenness of their space distribution (e.g., enhancing of space density of particles behind the moving planetesimal, Safronov 1958), deviation of initial particles velocities from the zero, increase of asteroid mass and density during the accretion of falling particles, and gradual diminution

of space density of the matter around the asteroid with time should be taken into account. Nevertheless, some qualitative results and conclusions obtained in this simplified simulation would still be applicable to some real systems. Namely, the results obtained here are valid if for every size range of particles their space distribution is nearly uniform and their velocities are nearly zero with respect to the asteroid center. Then the fall of bodies will slow down the asteroid rotation (not affecting the direction of angular momentum of the asteroid), and at a given density of the asteroid, the ratio of the number of particles impacting its leading sides to that for trailing sides will be (independent of the particles size range and their space density) determined by the value of the asteroid spin rate (of course, while the falling bodies are small enough compared with the asteroid itself). A different approach to the problem, which contains theoretical considerations on topographical changes on ellipsoidal or dumb-bell shaped asteroid surfaces due to cratering by falling particles can be found in Ronca & Furlong (1977, 1979). The authors suppose that the flux of meteoroids, as seen by an asteroid, is isotropic. This model is proper (in contrast to the model adopted in the present study) for the current solar system state (especially for tumbling asteroids).

2. General equations

We define a body-fixed coordinate frame in the asteroid. The axes x, y, z lie along the largest, intermediate and the shortest dimension correspondingly. The asteroid rotates uniformly around its largest moment of inertia, thus it rotates about its shortest z axis. Given a constant density ρ for the asteroid, there is a classical formula for the gravitational potential of a triaxial ellipsoid with respect to a unit mass particle (Subbotin 1949; Duboshin 1961):

$$V = k^2\pi\rho abc \int_{\lambda}^{+\infty} \left(1 - \frac{x^2}{a^2+s} - \frac{y^2}{b^2+s} - \frac{z^2}{c^2+s}\right)\frac{\mathrm{d}s}{R(s)} \qquad (1)$$

where $a > b > c$ are semiaxes of the ellipsoid, k is the Gauss constant, ρ is the asteroid density,

$$R(s) = \sqrt{(a^2+s)(b^2+s)(c^2+s)}, \qquad (2)$$

and λ is determined from the cubic equation

$$\frac{x^2}{a^2+\lambda} + \frac{y^2}{b^2+\lambda} + \frac{z^2}{c^2+\lambda} = 1. \qquad (3)$$

The potential of a dumb-bell asteroid is:

$$V = k^2 M\left(\frac{1}{r_1} + \frac{1}{r_2}\right), \qquad (4)$$

where r_1 and r_2 are the distances from a particle to the centers of dumb-bell spheres of mass M. The particle motion equations in a rotating body-fixed frame are the following (Subbotin 1937):

$$\ddot{x} - 2\omega\dot{y} = \Omega_x \qquad (5)$$

$$\ddot{y} + 2\omega\dot{x} = \Omega_y \qquad (6)$$

$$\ddot{z} = \Omega_z, \qquad (7)$$

where ω is rotation rate of the asteroid, and

$$\Omega = \omega^2(x^2+y^2)/2 + V. \qquad (8)$$

A particle moving is governed by equations of its motion (5)–(7) in a body-fixed frame (where the potential is computed using Eqs. (1) and (4)). The equations were solved numerically and integration was terminated when a particle had collided with any point of the surface of the ellipsoid or either of the lobes of the dumb-bell. The positions and velocities of nearly 33000 falling particles were computed at the points of collision with the asteroid surface. The triaxial ellipsoid asteroid model was chosen so that its semi-axes 28, 12 and 10.5 km, density of 2.5 g cm^{-3} and rotation period 4.63 hour were equal to those for asteroid 243 Ida (Beatty 1995; Matthew 2002) and the dumb-bell shaped model was chosen to be of the same mass as the ellipsoidal one. To study the dependence of distribution of zones subjected to the most intensive bombardment, the value of the asteroid spin period was varied from 0.2 hour to 365 days. Initially, particles filled uniformly a spherical layer between 200 and 1000 km from the asteroid center. The space density of particles was chosen so as to provide accumulated height of a few cm per a year over the asteroid surface (Ruzmaikina et al. 1989).

3. Results

Figures 1 and 2 demonstrate the projections of impact points on the equatorial plane of the asteroid. It should be noticed that while for the resting ellipsoid (Batrakov & Vasilkova 1997) the most bombarded areas are placed around the smallest and intermediate axes ends (where the impact velocities also are proved to be higher), the position of such areas for the rotating ellipsoid is quite different and depends on the value of the asteroid rotation period. This dependence is more distinct at shorter rotation periods. Figure 1 shows the absence of impact points at the longest ends of the trailing sides of an ellipsoidal asteroid at a spin period of 1.1 hour. In Fig. 2 a similar picture is drawn for an asteroid of dumb-bell shape of the same mass. Note that the case of spin period of 1.1 hour is taken as idealized marginal case just to demonstrate the effect of fast rotation on the distribution of impact points. Though, the asteroids of a dumb-bell or an ellipsoidal shape rotating so fast are not likely to exist physically. It can be shown that at spin periods shorter than 4.17 hour the centripetal acceleration for the lobes of our dumb-bell asteroid exceeds the acceleration of their attraction. (These would get balanced only at the densities higher than 36 g cm^{-3} (see also Burns 1975 for discussion of asteroid strengths).)

The impact points of possible erosion at short rotation periods are plotted in Figs. 3 and 4 as projections on the equatorial plane of the asteroids of ellipsoidal and dumb-bell shapes. While the zones occupy only a half of the surface of the ellipsoidal asteroid, they occupy almost the whole surface of the dumb-bell one of the same mass at the same rotation period. At the real period of rotation of asteroid Ida (of 4.63 hour) the

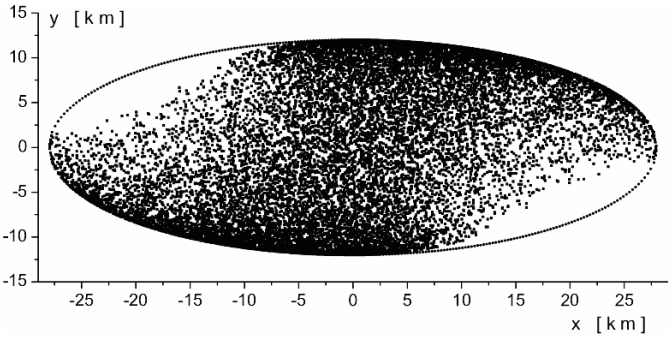

Fig. 1. Projections of impact points onto the asteroid equatorial plane. Period of rotation is equal to 1.1 hour. Viewing the asteroid looking down on the north pole. Trailing sides are at the left upper and right lower quarters of the picture.

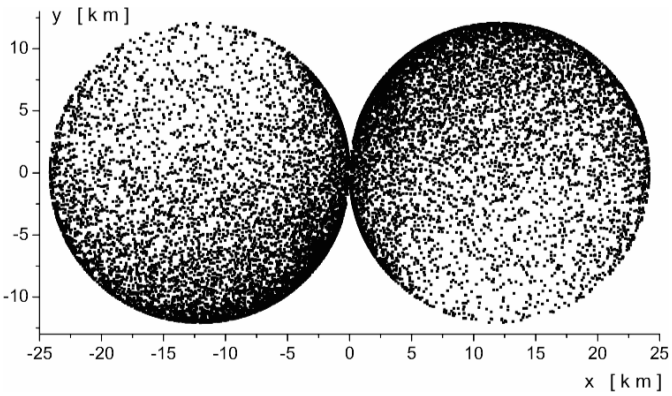

Fig. 2. Projections of impact points onto the asteroid equatorial plane. Period of rotation is equal to 1.1 hour. Viewing the asteroid looking down on the north pole. Trailing sides are at the left upper and right lower quarters of the picture.

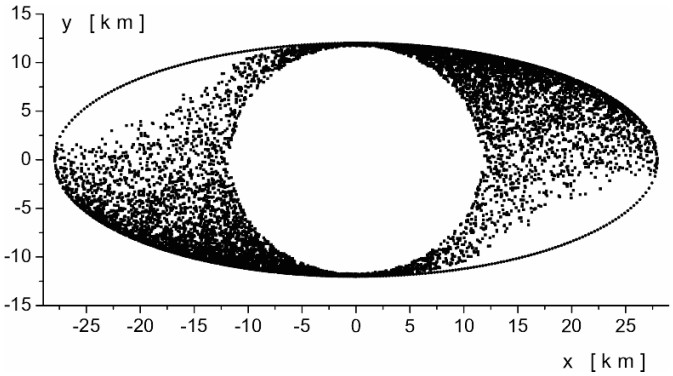

Fig. 3. Projections of points of possible erosion onto the asteroid equatorial plane. Rotation period is of 1.1 hour. Viewing the asteroid looking down on the north pole. Trailing sides are at the left upper and right lower quarters of the picture.

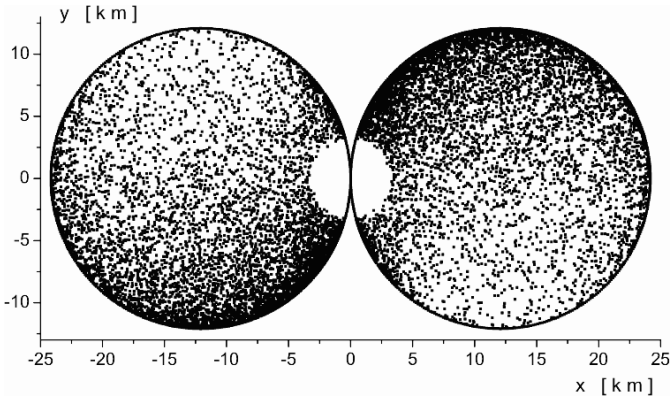

Fig. 4. Projections of points of possible erosion onto the equatorial plane of asteroid. Rotation period is of 1.1 hour. Viewing the asteroid looking down on the north pole. Trailing sides are at the left upper and right lower quarters of the picture.

erosion zones disappear on the ellipsoidal asteroid but still occupy about a half of the surface of a dumb-bell one (Fig. 5). The computations show that dumb-bell asteroids are subjected to erosion at periods of rotation up to 9 hours. For the same period (where comparable), dumb-bell asteroids are subjected to erosion more intensively. Figure 6 shows that even for a spherical shape and idealized clean surface, at rotation periods approaching the instability limit removal of particles from the surface is still possible. In this case the erosion zones are located at the band around the equator, causing poleward growth (Hartmann 1978). To compute the erosion zones the criterion was used described in Hartmann (1978) where shattering in a vacuum on a clean, coherent rock target at impact velocities 30 to 50 m s^{-1} indicates a spread of fragment velocities usually of 0.1 to 0.7 time the impact velocity. (The similar range of velocities was found at integration in the present simulation. The maximum values of relative impact velocities at a spin period of 1.1 hour approached 46 m s^{-1} for both models, and, at a spin period of 4.63 hour, was 18.5 m s^{-1} for ellipsoid and 28 m s^{-1} for dumb-bell models correspondingly.) So, choosing the best conditions to achieve erosion (which involve clean, smooth surfaces and the maximum possible rebound velocity), we considered the impact point as a point of possible erosion if

$$0.7\, v_{\rm impact} \geq v_{\rm escape}, \tag{9}$$

where $v_{\rm impact}$ is impact velocity of a particle and $v_{\rm escape}$ is escape velocity at a point of impact

$$v_{\rm escape} = \sqrt{2V} \tag{10}$$

and formulae (1) and (4) were used to compute potential V at the point of collision of a particle with the surface. But the above "best" case is unrealistic in several ways (Hartmann 1978). The earliest planetesimals (and particles themselves) are not the polished igneous spheres used for experiments by Hartmann (1978). They have regolith-covered surfaces, or consist entirely of loose aggregates of primitive materials (Hartmann 1978; Housen et al. 1979; Ruzmaikina et al. 1989, etc.). This regolith would ensure additional energy loss. A regolith depth of only about 0.04 projectile diameter would cut the velocity of rebound to

$$v_{\rm rebound} = 0.4\, v_{\rm impact} \tag{11}$$

and a regolith of a depth comparable to the projectile diameter virtually stops the projectile (as experiments by Hartmann 1978 on low-velocity impacts in a vacuum showed). So, the value of the rebound velocity strongly depends on both the thickness of the asteroid regolith layer and size of the projectile.

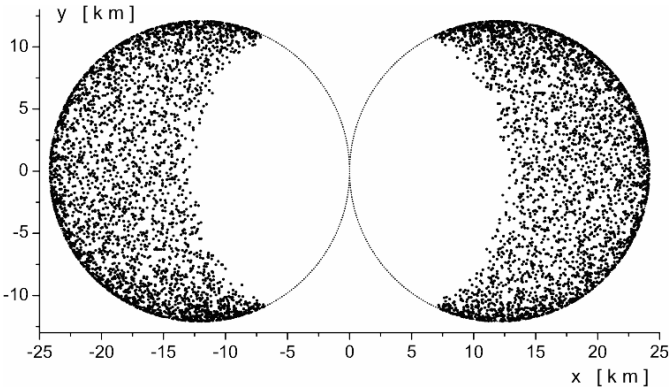

Fig. 5. Projections of points of possible erosion onto the equatorial plane of asteroid. Rotation period is of 4.63 hour. Viewing the asteroid looking down on the north pole. Trailing sides are at the left upper and right lower quarters of the picture.

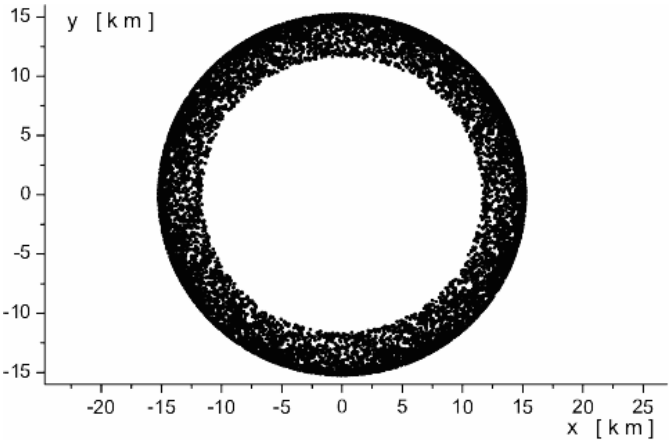

Fig. 6. Projections of points of possible erosion onto the equatorial plane of a sphere asteroid for the case of a clean solid surface. Rotation period is of 1.1 hour. Viewing the asteroid looking down on the north pole.

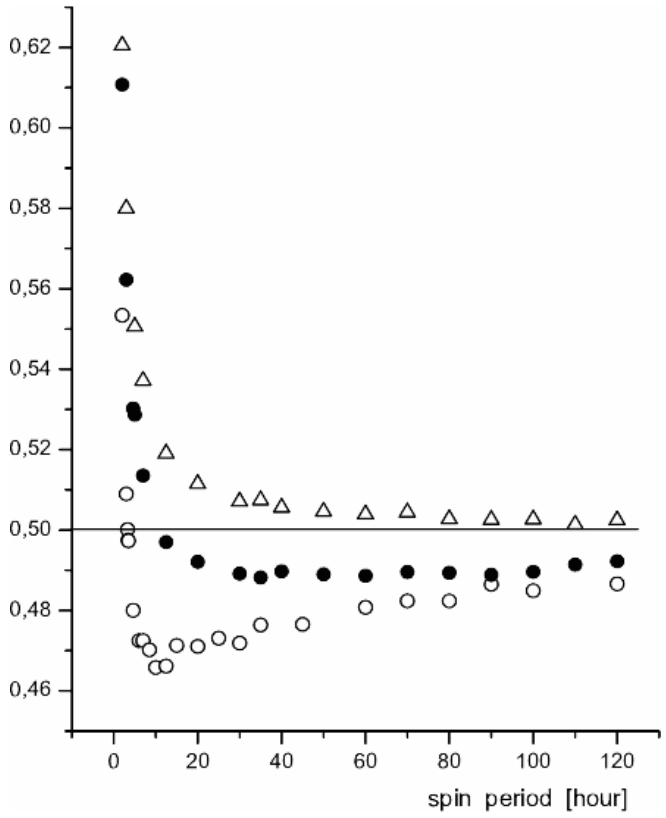

Fig. 7. The fraction of the total number of impacting particles falling on to the leading sides of the asteroid depending on the asteroid rotation period. Particles initially are distributed uniformly inside a spherical layer 200 to 1000 km from the asteroid center. The following models of gravitational attraction of particles are considered (from the upper curve to the lower one): (1) the asteroid of triaxial ellipsoid shape with the semiaxes 28, 12, 10.5 km attracts like a sphere of the same mass; (2) the asteroid has the triaxial ellipsoid shape above and its potential is expressed by Eq. (1); (3) the asteroid of the same mass has dumb-bell shape and its potential expressed by Eq. (4).

In present simulation our models gain a regolith layer of a few cm per a year (Ruzmaikina et al. 1989), so, we would expect them to be covered with a multimeter regolith layer. Then the velocity of rebound would be damped to nearly zero. So, for early accretionary stage considered in this study, the assumption of no rebounds at impact seems more reasonable than that of further re-ejection and redistribution of ejecta over the asteroid surface. (In particular, it means that every particle has a single point of impact and, so, a single point in Figs. 1–6). Therefore, if there is no erosion, the zones of the most intensive bombardment (Figs. 1 and 2) become regions of the most intense accretion. Of course, if rebounds were taken into account (e.g., in the case of clean non-regolith-covered surface), the regions of the most intense bombardment would be slightly shifted, especially at fast rotation.

It seems that at fast rotation the predominant shifting would occur in the direction opposite to that of asteroid spinning, that is (looking, for example, at the upper half of Figs. 1 and 2) to the right of the leading side. On the other hand, at the same time new particles coming from the left regions (including those of the trailing sides) would partly compensate the leaving ones. Computations show that if the condition (11) is satisfied (that is in the case of regolith-covered surfaces), the erosion is possible only for dumb-bell shaped asteroids and only at rotation periods shorter than 1.1 hour. So, as this range of spin period is not common for the asteroids of dimensions considered, in fact, erosion was impossible for asteroid planetesimals of both ellipsoidal and dumb-bell shapes and all falling particles were being accumulated on the asteroid surfaces. In Fig. 7, dependence of the fraction of particles bombarding the leading sides of the asteroid (with respect to the total number of falling particles) on the asteroid rotation period is represented for 3 different cases of an attracting gravitational field of the asteroid (from upper curve to lower): 1) it is assumed that the asteroid of ellipsoid shape attracts like a sphere of the same mass, that is, the particles fly along the straight line towards the ellipsoid center and the coordinates at points of collission of particles with the rotating ellipsoid are computed; 2) the gravitational potential of the asteroid of triaxial ellipsoid shape is computed using Eq. (1); 3) falling of particles to the dumb-bell shaped asteroid of the same mass is governed by the gravitational field of a dumb-bell asteroid (Eq. (4)). The following conclusions can be made. At first, there is a certain value of the rotation period (at the density

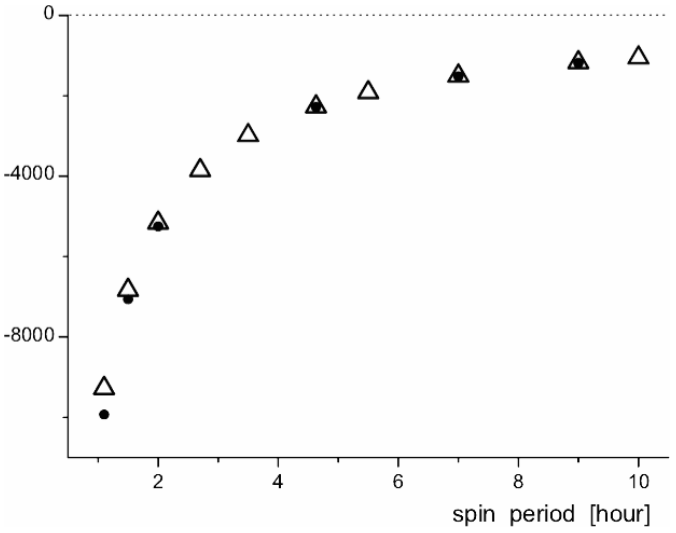

Fig. 8. Combined contribution to the angular momentum of the asteroid from all impacting particles via the asteroid rotation period: for the asteroid of triaxial ellipsoid shape with semi-axes 28, 12, 10 km (circles) and for a dumb-bell shaped asteroid of the same mass (open triangles).

and dimensions chosen in the current study, it is approximately equal to 9.1 hour for the ellipsoid model and 3.3 hour for the dumb-bell one) such that at shorter periods the number of particles falling to the leading sides is greater than the number of those impacting the trailing sides. Second, this phenomenon is the consequence of the specific influence of the triaxial ellipsoid gravitational field only – not the "geometrical" result of its elongated shape (see the curve corresponding to the case 1): the asteroid has a triaxial ellipsoid shape but its attraction is central; as a result, the predominance of the number of particles impacting the leading sides with respect to trailing ones exists for all values of the asteroid rotation period). Figure 8 reflects the combined contribution of all impacting particles to the angular momentum of ellipsoidal and dumb-bell asteroids via the asteroid rotation period:

$$\Delta \boldsymbol{H} = \sum m\, \boldsymbol{r} \times \boldsymbol{v}. \tag{12}$$

Here m, $\boldsymbol{r}$, $\boldsymbol{v}$ are the particle mass, radius-vector and relative velocity at the impact point. Figure 8 shows that at all values of rotation period the falling out of particles damps rotation of asteroids of both shapes.

4. Conclusions

The computations described above were repeated for different sizes of particles and at different space densities. Density of the asteroid itself was varied also. These computations showed that: (1) for an asteroid of either shape (a triaxial ellipsoid of any elongation and a dumb-bell of the same mass) the flux of particles impacting the leading sides of the asteroid is higher than that for its trailing sides if the spin period of the asteroid is shorter than certain value (for ellipsoid model with semi-axes 28, 12, 10.5 km and density of 2.5 g cm^{-3} and for the dumb-bell model of the same mass these values are approximately equal to 9.1 and 3.3 hour respectively). The more the shape of the asteroid is elongated (or the density less), the longer is the mentioned value of the period. The shape evolution will have an asymmetrical character, forming some excrescences at the leading sides (at areas corresponding to the zones of the most intensive bombardment in Figs. 1 and 2) until the period of rotation is less than the value of the period at which leading and trailing sides receive equal flux of impacting particles (in Fig. 7 it corresponds to a period at which the curve $y = 0.5$ crosses any other curve). At the same mass and spin period the excrescences will be more distinct and stick out more for ellipsoidal asteroids than for dumb-bell shaped ones, especially at fast rotation. It seems that at a nearly uniform space distribution of particles (for any size range) and their low relative velocities, both the ellipsoidal and dumb-bell asteroids at short periods of rotation tend to look like asymmetrically knitting together spheres with excrescences near the rotation axis at the leading sides of the asteroid. At long spin periods the zones of the most intense bombardment are located for the ellipsoid in areas around the rotation axis and around the ends of the small axis of the asteroid equator (see also Batrakov & Vasilkova 1997), and for dumb-bell asteroids, near the point of contact. Therefore, at long periods, triaxial ellipsoids will tend to adopt the shape of ellipsoids of rotation and further, approaching it, will tend to adopt the shape of a sphere. So, both the triaxial ellipsoid and dumb-bell asteroids will tend to adopt a spherical shape. (2) Independent of the space density of particles and their masses (of course, until they are much smaller than the asteroid's), the effect of slowing down the rotation rate of an asteroid is always valid for uniformly distributed particles of the same mass. The masses and space density of particles only affect the drag rate but not the direction of rotation. Also, the shorter the period of asteroid rotation the steeper the curve in Fig. 8 and, therefore, the stronger the damping of asteroid rotation. Note that the plotted value of angular momentum contribution in Fig. 8 is a z component of the combined angular momentum contribution vector, as computations show that its x and y components are nearly zero. This damping effect is similar to a drag effect described for the model of Harris in Davis et al. (1979) though being for the early stage of accretion. (In the current solar system, where collisions between asteroids are common due to high eccentricities of their orbits, it is clear that just the rarer collisions with large bodies will determine whether the asteroid will be spinning up, damping or changing the sense of rotation). (3) The computation of possible erosion zones has led to a conclusion (not new (Harris 1977; Hartmann 1978; Housen et al. 1979, etc.), that the largest bodies in the swarm would accumulate regolith. The zones accreting the mass more intensively are those where the bombardment is more intense (see Figs. 1 and 2).

Acknowledgements. I would like to thank the referee Dr. Joseph Spitale for helpful criticism and valuable advices.

References

Batrakov, Yu. V., & Vasilkova, O. 1997, On Possible Erosion of an Asteroid in a Dust Cloud. Computer Methods of Celestial Mechanics, November 18-20, 1997, Abstracts of the Conference

Beatty, J. K. 1995, Ida & Company, Sky Telesc., January, 20-23
Bell, E. F., Davis, D. R., Hartmann, W. K., & Gaffey, M. J. 1989, The Big Picture, in Asteroids II, ed. R. P. Binzel, T. Gehrels, & M. S. Matthews (Univ. of Arizona Press), 921
Burns, J. A. 1975, Icarus, 25, 545
Davis, D. R., Chapman, C. R., Greenberg, R. J., Weidenschilling, S. J., & Harris, A. W. 1979, Collisional Evolution of Asteroids: Populations, Rotations and Velocities, in Asteroids, ed. T. Gehrels (Univ. of Arizona Press), 528
Duboshin, G. N. 1961, Theory of Gravitation Attraction (Moscow), 288 (in Russian)
Harris, A. W. 1977, Icarus, 31, 168
Hartmann, W. K. 1968, ApJ, 152, 337
Hartmann, W. K. 1978, Icarus, 33, 50
Housen K. R., Wilkening L. L., Chapman C. R., & Greenberg R. J. 1979, Regolith Development and Evolution on Asteroids and the Moon, in Asteroids, ed. T. Gehrels (Univ. of Arizona Press), 601
Matthew, D. 2002, Astronomy today: Asteroids, http://www.astronomytoday.com/astronomy/asteroids.html
Ronca, L. B., & Furlong, R. B. 1977, The Moon, 17, 233
Ronca, L. B., & Furlong R. B. 1979, Moon and the Planets, 21, 409
Ruzmaikina, T. V., Safronov, V. S., & Weidenschilling, S. J. 1989, Radial Mixing of Material in the Asteroidal Zone, in Asteroids II, ed. R. P. Binzel, T. Gehrels, & M. S. Matthews (Univ. of Arizona Press), 681
Ruskol, E. L., & Safronov, V. S. 1998, Astron. Vestnik, 32, 291 (in Russian)
Safronov, V. S. 1958, Voprosi Kosmogonii, 6, 63 (in Russian)
Safronov, V. S. 1972, Evolution of the Protoplanetary Cloud and Formation of the Earth and the Planets, NASA TT-677
Subbotin, M. F. 1937, Manual on Celestial Mechanics, II (Moscow), 404 (in Russian)
Subbotin, M. F. 1949, Manual on Celestial Mechanics, III (Moscow), 280 (in Russian)